S1 Main processes and related parameters in the AUTOSHED

The AUTOSHED adopts the rain-on-grid approach for pluvial flood simulation where surface runoff generation and routing processes are sequentially simulated on triangular-shaped meshes. For rainfall-runoff simulation, AUTOSHED considers the typical hydrological processes including building interception, vegetation interception, and soil infiltration as follows:

- Building drainage is parameterized as follows:

$$q_b = \begin{cases} 0, H_b < d_b \\ D_{0,b}\left(H_b - d_b\right)^{b_b}, H_b \geq S_{b,\max} \end{cases} \tag{1}$$

where q_b is the building drainage rate ($\mathrm{mm \cdot h^{-1}}$), H_b is the accumulated runoff depths on the building roof (mm), $D_{0,b}$, b_b, $S_{b,\max}$ are the corresponding drainage coefficients and set as: $D_{0,b} = 10\ \mathrm{mm \cdot h^{-1}}$, $b_b = 3$, $S_{b,\max} = 1\ \mathrm{mm}$ by default (Järvi et al., 2011; Cao et al., 2021).

- Vegetation drainage is parameterized as follows:

$$q_t = \begin{cases} 0, H_t < S_{t,\max} \\ D_{0,t} e^{b_t(H_t - d_t) - 1}, H_t \geq S_{t,\max} \end{cases} \tag{2}$$

where q_t is the vegetation drainage rate ($\mathrm{mm \cdot h^{-1}}$), H_t is the accumulated runoff depths on the tree canopy (mm), $D_{0,t}$, b_t are the corresponding drainage coefficients and set as: $D_{0,t} = 0.013\ \mathrm{mm \cdot h^{-1}}$, $b_t = 1.71$ by default (Järvi et al., 2011) and $S_{t,\max}$ is the maximum interception of the vegetation canopy (mm) parameterized by the leaf area index LAI according to the A.P.J. DE ROO model (De Roo et al., 1996):

$$S_{t,\max} = 0.935 + 0.498 \cdot \mathrm{LAI} - 0.00575 \cdot \mathrm{LAI}^2 \tag{3}$$

- Soil infiltration is solved from the finite difference solution of the Richards equation (Ni et al., 2008). The related soil hydraulic properties are derived from the HiHydroSoil v2.0 database (Simons et al., 2020). The soil infiltration is only considered in the pervious part of each triangular-shaped unit whose impervious ratio is set according to the land-use-based empirical values (BMCPNR, 2022), as summarized in the Table S1.

After obtaining surface runoff, AUTOSHED solves the full two-dimensional shallow water equations (SWEs) for flood routing. The SWEs only have one parameter, the Manning coefficient, which is set according to the land-use-based empirical values (BMCPNR, 2022), as summarized in the Table S1.

Table S1. Key parameters of the AUTOSHED model by land use type.

Parameter	Tree	Grassland	Cropland	Built area	Bareland	Water
Impervious ratio	0.05	0.05	0.05	1	0.8	1
Manning coefficient	0.08	0.05	0.06	0.015	0.03	0.02

S2 Radar-based accumulated rainfall field

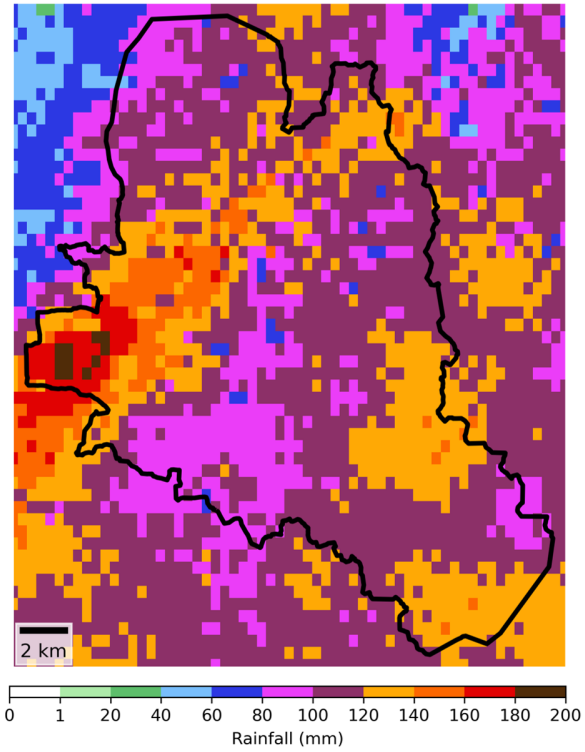

Figure S1. Radar-based accumulated rainfall field between 21:00 on 8 August and 09:00 on 10 August in the Beijing Municipal Administrative Center.

S3 Rainfall–temperature scalings for mean areal rainfall and rainfall-affected area

Table S2. Rainfall–temperature scalings (% $°C^{-1}$) for mean areal rainfall (MAR), rainfall-affected area (Area), and coefficient of variation (CV) in different MAR intensity groups.

MAR group	5th	10th	15th	20th	25th	30th	35th	40th	45th	50th	55th	60th	65th	70th	75th	80th	85th	90th	95th	99th
MAR	-1.2	-1.1	-1.0	-0.7	-0.8	-0.6	-0.5	-0.3	0	0.1	0.2	0.3	0.6	0.8	0.9	1.1	1.6	1.9	2.7	3.6
Area	-1.8	-2.3	-0.5	-1.1	-1.7	-1.0	-0.5	-1.1	-1.1	-2.2	-1.0	-1.9	-2.4	-2.3	-2.3	-2.0	-2.1	-1.5	-1.5	-0.9
CV	0.7	0.9	0.7	0.9	1.5	0.7	0.4	1.0	1.3	1.2	1.1	1.2	2.0	1.7	1.8	1.3	1.1	1.4	0.9	0.9

S4 Validation of RainyDay

Table S3. Validation of mean rainfall return levels from RainyDay against that from station observations.

Return levels ($mm\,h^{-1}$)	2yr	5yr	10yr	30yr	50yr	100yr
SST	34	47	53	60	64	68
Stations	35	48	55	64	67	71
Bias	3%	2%	4%	6%	5%	4%

S5 Inundation duration in the Beijing Municipal Administrative Center under 100-yr return level storms

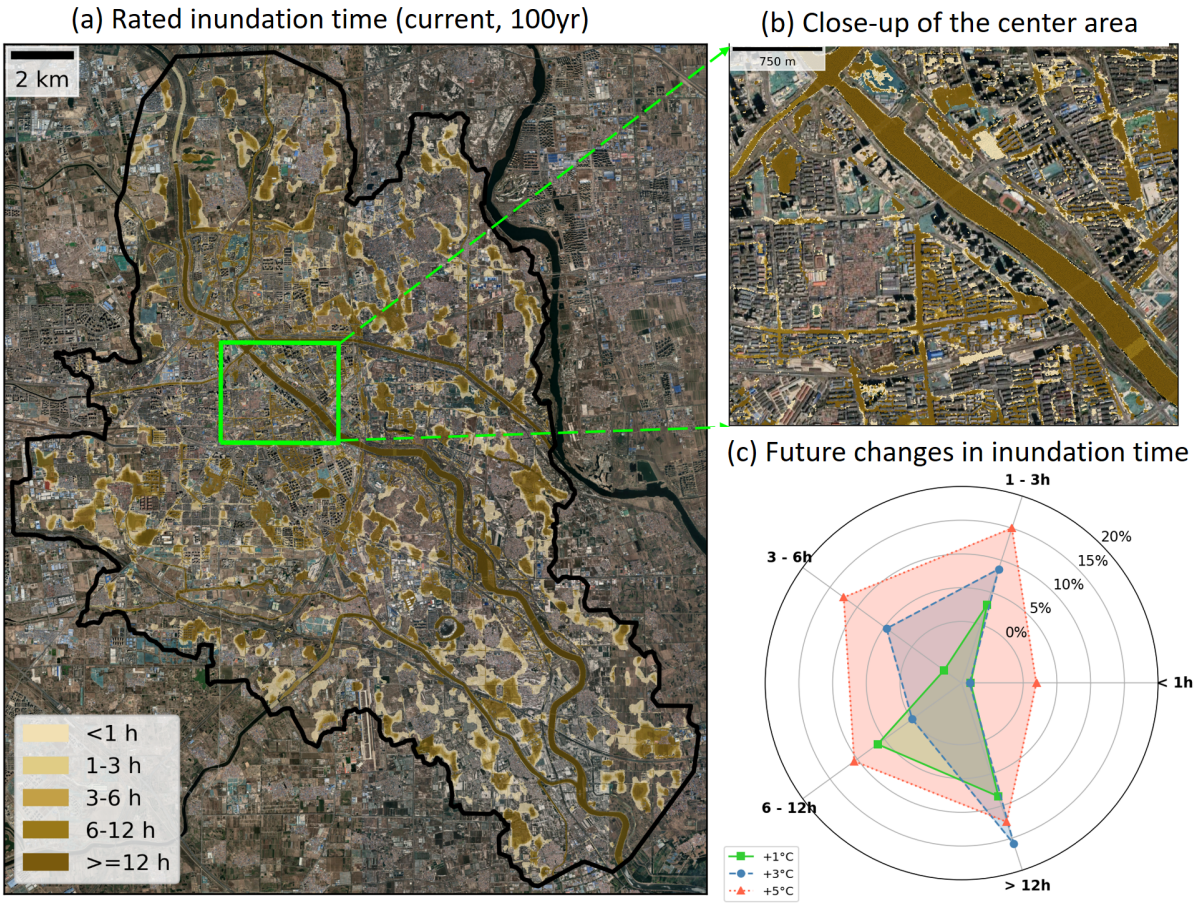

Figure S2. (a) The rated inundation duration of 100-year return level under the current climate, (b) Close-up at the BMC centre, and (c) its projected future changes in different hazard levels within BMC under different warming conditions. Basemaps are derived from ESRI World Imagery (Credit: Esri, TomTom, Garmin, FAO, NOAA, USGS, © OpenStreetMap contributors, and the GIS User Community).

S6 Spatial resolution impact on future urban floods

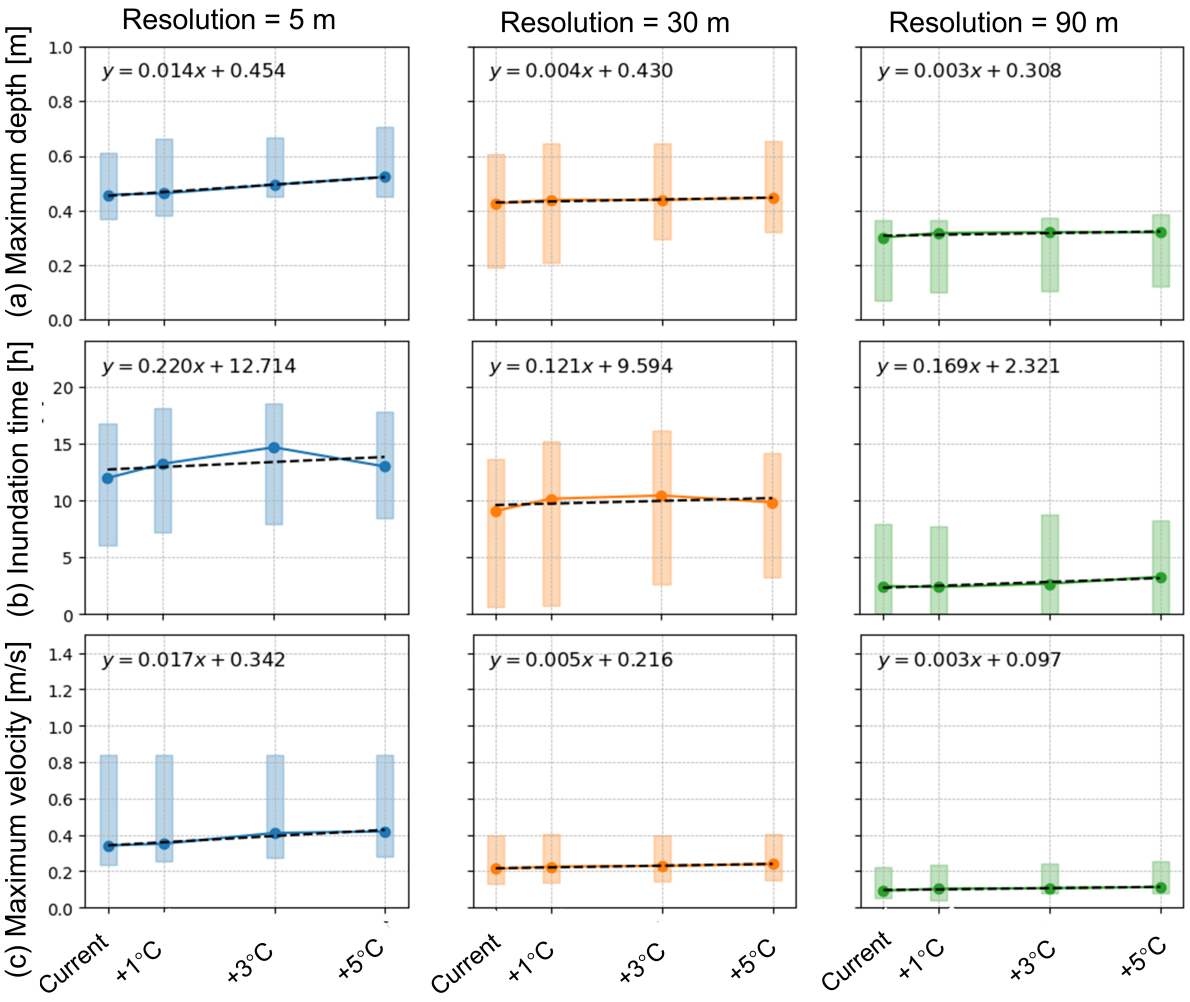

Figure S3. Impact of spatial resolution on future changes in (a) maximum inundation depth, (b) inundation time, and (c) maximum velocity at local flood-prone points under different warming scenarios.

References

BMCPNR: the Technical Specification for Construction and Application of Mathematical Model of Urban Flooding Prevention and Control System, DB11/T 2074-2022, Beijing Municipal Commission of Planning and Natural Resources, Beijing, China, in Chinese, 2022.

Cao, X., Qi, Y., and Ni, G.: Significant Impacts of Rainfall Redistribution through the Roof of Buildings on Urban Hydrology, Journal of Hydrometeorology, 22, 1007 – 1023, https://doi.org/10.1175/JHM-D-20-0220.1, 2021.

De Roo, A., Wesseling, C. G., Jetten, V. G., and Ritsema, C. J.: LISEM: A physically-based hydrological and soil erosion model incorporated in a GIS, IAHS Publication, 235, 395–403, 1996.

Järvi, L., Grimmond, C., and Christen, A.: The Surface Urban Energy and Water Balance Scheme (SUEWS): Evaluation in Los Angeles and Vancouver, Journal of Hydrology, 411, 219–237, https://doi.org/10.1016/j.jhydrol.2011.10.001, 2011.

Ni, G.-H., Liu, Z.-Y., Lei, Z.-D., Yang, D.-W., and Wang, L.: Continuous Simulation of Water and Soil Erosion in a Small Watershed of the Loess Plateau with a Distributed Model, Journal of Hydrologic Engineering, 13, 392–399, https://doi.org/10.1061/(ASCE)1084-0699(2008)13:5(392), 2008.

Simons, G., Koster, R., and Droogers, P.: Hihydrosoil v2. 0-high resolution soil maps of global hydraulic properties, FutureWater Report, https://www.futurewater.eu/projects/hihydrosoil, 2020.